Rapid Communications

Interlayer exchange coupling in Pt/Co/Ru and Pt/Co/Ir superlattices

Sabit Karayev,[1] Peyton D. Murray,[2] Durga Khadka,[1] T. R. Thapaliya,[1] Kai Liu,[2,3] and S. X. Huang[1,*]

[1]*Department of Physics, University of Miami, Coral Gables, Florida 33146, USA*

[2]*Department of Physics, University of California, Davis, California 95616, USA*

[3]*Department of Physics, Georgetown University, Washington, D.C. 20057, USA*

(Received 31 December 2018; published 8 April 2019)

Magnetic multilayer thin films with perpendicular magnetic anisotropy (PMA) and interfacial Dzyaloshinskii-Moriya interaction (iDMI) are of intense interest for realizing magnetic skyrmions and modifying topological spin textures. We systematically investigate interlayer exchange coupling (IEC) in Pt/Co/Ru(Ir) superlattices that have PMA and large iDMI. The IEC is greatly tunable by varying Ru(Ir) or Pt thickness and the antiferromagnetic IEC is as large as 1.3 $\mathrm{mJ/m^2}$ that is on the same order of magnitude as the iDMI. We find unusual magnetic hysteresis loop crossing between field-ascending and -descending magnetization curves. Furthermore, we identify magnetic phase diagrams for antiferromagnetic IEC and hysteresis loop crossing with respect to Ru(Ir) and Pt thickness. Our experimental findings may open a way in the development of synthetic antiferromagnetic spintronics and/or the realization of antiferromagnetic skyrmions.

DOI: 10.1103/PhysRevMaterials.3.041401

Magnetic skyrmions were discovered in 2009 [1] in bulk crystals of special magnets called the chiral B20 magnets (MnSi, FeGe, etc.), which have noncentrosymmetric crystal structures with broken inversion symmetry and low Curie temperatures (T_C) below room temperature. As a result, in B20 magnets, in addition to the symmetric Heisenberg exchange interaction, there is also a nontrivial antisymmetric Dzyaloshinskii-Moriya interaction (DMI) $H_{\mathrm{DM}} = \mathbf{D}_{ij} \cdot (\mathbf{S}_i \times \mathbf{S}_j)$, where $\mathbf{D}_{ij}$ is the Dzyaloshinskii-Moriya vector and its direction depends on the symmetry. DMI is key to realizing magnetic skyrmions. Recent focus on skyrmions has been on the search for skyrmions in multilayer thin films or nanostructures using common ferromagnets such as Co with a simple crystal structure and T_C well above room temperature [2]. The strategies include imprinting a magnetic vortex on magnetic multilayer films with perpendicular magnetic anisotropy (PMA) [3–5] and introducing large interfacial DMI (iDMI) in asymmetric magnetic multilayer thin films [6–10]. In the latter case, the multilayer usually has a structure of HM1/FM/HM2, where FM is a ferromagnet and HM is a heavy metal, that has broken inversion symmetry and large spin-orbit coupling [6]. The large iDMI favors a rapid rotation of the spins in multilayer films with PMA and can stabilize skyrmions [6]. Many multilayer thin films [7–10] with PMA and large iDMI, such as the Pt/Co/Ir multilayer, have been demonstrated to realize skyrmions at room temperature.

In B20 magnets and multilayer films with PMA and iDMI, the two-dimensional (2D) skyrmions with the same polarity (i.e., ferromagnetically coupled) form a lattice (or disordered structures) in a plane. Each skyrmion plane couples ferromagnetically with its neighboring planes [11]. When those skyrmions are driven by an electric current, their motion deviates from the current direction. The transverse motion is called the skyrmion Hall effect. There is increasing interest to realize antiferromagnetic skyrmions [or antiferromagnetically coupled skyrmions (AFM-Skx)] which can move along the current direction without the skyrmion Hall effect, such as in certain antiskyrmion systems [12–14]. AFM-Skx may be realized in antiferromagnets with DMI [15] or multilayer skyrmions that are coupled antiferromagnetically [16], as proposed in theories. Very recently, ferrimagnetic skyrmions has been realized in ferrimagnet GdFeCo with small skyrmion Hall effect [17], while AFM-Skx has yet to be realized [18].

In magnetic multilayer films, in addition to PMA and iDMI, interlayer exchange coupling (IEC) [19–22] can also be introduced in FM1/NM/FM2 and tuned over a wide range, where NM is a nonmagnetic metal such as Ru. IEC shows an oscillation with the thickness of NM and can be antiferromagnetic (AFM-IEC) or ferromagnetic (FM-IEC). AFM-IEC is of particular interest and is key to realizing synthetic antiferromagnets (SAF) that are crucial components to develop synthetic antiferromagnetic spintronics [23,24]. Among the transition metals, Ru has the largest antiferromagnetic exchange coupling strength (J_{AF}) of up to 5 $\mathrm{mJ/m^2}$, while it is zero for Pt [19]. There are few results in experiments [25] and simulations [26] showing that the FM-IEC can stabilize skyrmions at a zero magnetic field. In these studies, the FM-IEC is small, and acts to provide a stray field in the absence of an external magnetic field. Simulations also show structural transitions of skyrmion lattices in magnetic films with iDMI and AFM-IEC [27].

Despite intense interest in iDMI and AFM-IEC, however, experimentally introducing large IEC in a magnetic multilayer while preserving PMA and large iDMI is not trivial and remains largely unexplored. In this work, we design magnetic superlattices and systematically study IEC in $[\mathrm{Pt/Co/Ru}]_N$ and $[\mathrm{Pt/Co/Ir}]_N$ superlattices that have PMA and large iDMI (Fig. 1). Although Co layers are separated by Ru(Ir) and Pt that has zero IEC, large oscillatory IEC can still be introduced.

*sxhuang@miami.edu

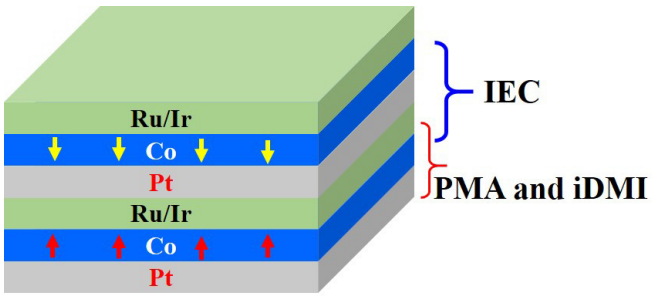

FIG. 1. Schematic diagram of Pt/Co/Ru(Ir) multilayer with PMA, iDMI, and IEC.

Furthermore, we observe unusual hysteresis loop crossing and identify phase diagrams for AFM-IEC and loop crossing.

Antiferromagnetically coupled multilayers of $[(Co/Pt)_{X\text{-}1}/Co/Ru]_N$ with PMA have been well studied [28,29], where X is much larger than 1. In this system ($[(Co/Pt)_{X\text{-}1}/Co/Ru]_N$ with large X), most Co layers are sandwiched by Pt layers and have symmetric interfaces, so that the net iDMI is expected to be small, if not zero. Interestingly, two distinct remanent states and reversal modes were observed. In mode 1, each magnetic layer reverses its magnetization independently (layer-by-layer switching so that several magnetic layers reverse their moments simultaneously). In mode 2, the reversal of magnetization is locally synchronized with ferromagnetic coupling along vertical directions. By tuning the material and/or geometrical parameters, isolated bubble domains can form at an applied field [30,31]. The bubble domains can be antiferromagnetic or ferromagnetic coupled between neighboring magnetic layers along the vertical direction.

$[Pt/Co/Ru]_N$ and $[Pt/Co/Ir]_N$ multilayer films are fabricated on Si substrates with 500 nm SiO_x by magnetron sputtering in a high vacuum system with base pressure better than 5×10^{-8} torr. Previously, we showed that both $[Pt/Co/Ru]_N$ and $[Pt/Co/Ir]_N$ ($N = 1,\ 2$) have large iDMI up to 2.66 mJ/m^2 and iDMI is nearly independent of Ru/Ir thicknesses [32]. In this work, magnetic superlattices $[Pt(10)/Co(8)/Ru(7)]_{10}$ (nominal thickness in parentheses has unit of Å), $[Pt(10)/Co(8)/Ru(wedge)]_N$ ($N = 5,\ 10$), $[Pt(10)/Co(10)/Ru(wedge)]_{10}$, $[Pt(wedge)/Co(8)/Ru(7)]_{10}$, and $[Pt(10)/Co(8)/Ir(wedge)]_N$ ($N = 3,\ 10$) are studied. All the multilayer films have a 30 Å Ru seed layer and a 30 Å Pt capping layer. The nominal thickness is estimated based on sputtering rates that are calibrated using thick films (30–60 nm, uniform or wedge films). Electrical contacts are made on unpatterned films by bonding 25 μm Al wires for anomalous Hall resistance measurements that are used to determine magnetic hysteresis curves. For the multilayer films in this work, all the Co layers are sandwiched by a Pt layer and a Ru/Ir layer, and therefore have asymmetric interfaces with large iDMI. This is the key difference between our films and $[(Co/Pt)_{X\text{-}1}/Co/Ru]_N$ that has been extensively studied [28].

Figure 2(a) shows a representative x-ray reflectivity measurement on a $[Pt(10)/Co(8)/Ru(7)]_{10}$ multilayer film. Two oscillations in the x-ray reflection intensity are observed, indicating the high quality of the superlattice. The oscillation with two broad peaks at around 3.75 ° and 7.4 °, respectively,

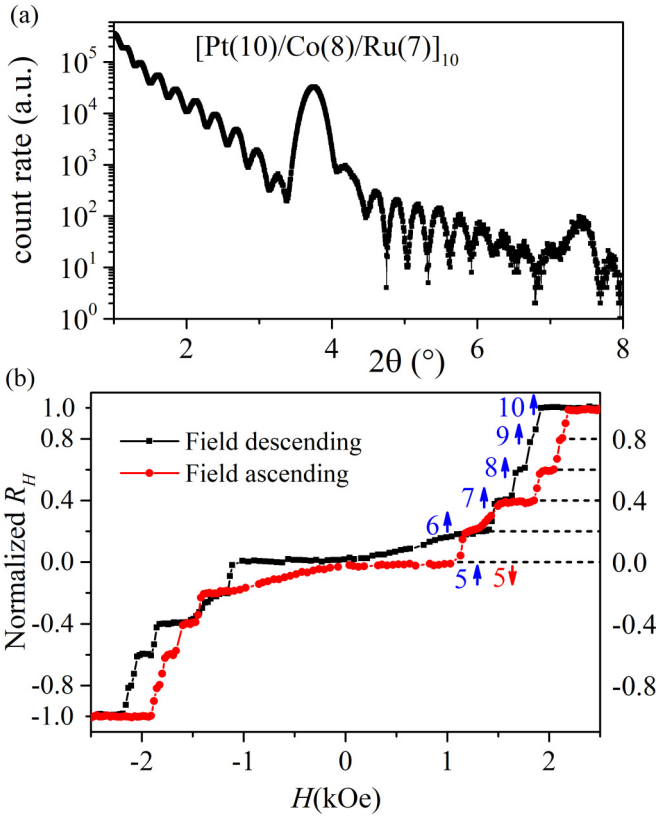

FIG. 2. X-ray reflectivity as a function of 2θ for $[Pt(10)/Co(8)/Ru(7)]_{10}$ superlattice. (b) Normalized Hall resistance of $[Pt(10)/Co(8)/Ru(7)]_{10}$ superlattice as a function of magnetic field for field descending (solid black squares) and ascending (solid red circles), respectively. Blue up (red down) arrows indicate moments pointing up (down).

originates from the diffraction of the superlattice base unit Pt(10)/Co(8)/Ru(7). The two broad peaks are separated by 3.65 °, corresponding to a thickness of 24.2 Å that agrees well with the designed thickness of 25 Å. The other periodic oscillation has a period of about 0.29 °, corresponding to total thickness of 304 Å, close to the designed thickness of 310 Å. The x-ray diffraction (XRD) reflectivity results demonstrate the high quality of superlattice structure with sharp interfaces that are important for IEC.

Figure 2(b) shows normalized Hall resistance (R_H) as a function of magnetic field for a $[Pt(10)/Co(8)/Ru(7)]_{10}$ multilayer. The magnetic hysteresis loop shows multiple Hall resistance plateaus—signatures of antiferromagnetic IEC (AFM-IEC). More interestingly, it shows an *exact single* layer-by-layer switch of magnetization. At zero field, $R_H \approx 0$, indicating that five Co layers have magnetic moments pointing up, while their neighboring Co layers have moments pointing down due to the AFM-IEC [Fig. 1 and Fig. 2(b)]. This zero-R_H state (five up, five down) remains unchanged along a field-ascending sweep until the field increases to 1130 Oe. At 1130 Oe, the system makes a sharp transition to the $R_H \approx 0.2$ state, suggesting that only one Co layer flips its moment and now six Co layers have moments pointing up. As the magnetic field further increases, the system makes transitions to the $R_H \approx 0.4$ state (seven up, three down) at 1430 Oe, the

$R_H \approx 0.6$ state (eight up, two down) at 1880 Oe, the $R_H \approx 0.8$ state (nine up, one down) at 2080 Oe, and the saturated state at 2200 Oe, respectively. These results indicate only one Co layer flips its moment at each transition (i.e., single layer-by-layer switching). It is interesting to note that the width of the resistance plateau (i.e., the field range where the $R_H = n/5$ state is stable) is different for different R_H states. The width is about 1130 Oe for the $R_H \approx 0$ state, 90 Oe for the $R_H \approx 0.2$ state, 350 Oe for the $R_H \approx 0.4$ state, 130 Oe for the $R_H \approx 0.6$ state, and 20 Oe for the $R_H \approx 0.8$ state, respectively. As the field decreases from a positive saturation field, the system makes similar single layer-by-layer switching to the $R_H \approx 0.2$ state at 1410 Oe. However, between the $R_H \approx 0.2$ state and $R_H \approx 0$ states, the system makes a smooth transition from 1130 Oe to zero field. More interestingly, between 1410 and 1130 Oe, the field-descending curve is below the field-ascending curve. This is different from the usual magnetic hysteresis loop in which the field-descending curve is always above the field-ascending curve. The unusual loop crossing is closely related to AFM-IEC, as discussed in detail later.

To investigate how the IEC can be tuned in a Pt/Co/Ru(Ir) multilayer with large iDMI, we fabricated wedged films in which only Ru(Ir) or Pt thicknesses vary continuously along 2" samples. We showed that iDMI remains nearly unchanged due to its interfacial origin when the thickness of nonmagnetic metals changes [32]. It is also known that PMA originates from the interface and is nearly independent of the thickness of nonmagnetic metal (e.g., the PMA of a Pd/Co multilayer is nearly a constant when Pd thickness is more than 5 Å [33]). IEC, on the other hand, strongly depends on the thickness of nonmagnetic metals. The Ru(Ir)/Pt wedged films allow one to introduce largely variable IEC into the magnetic multilayer films with essentially the same iDMI and PMA. Figures 3(a)–3(e) show representative normalized Hall loops for $[Pt(10)/Co(8)/Ru(wedge)]_{10}$ films with various Ru thicknesses indicated in the figures. Note the Hall resistances (i.e., magnetization) have quite different hysteresis loops (e.g., unusual loop crossing and single layer-by-layer switching) than those in $[(Co/Pt)_{X\text{-}1}/Co/Ru]_N$ [28] and $[Co/Ru]_{10}$ films [20] that have PMA but negligible iDMI, suggesting iDMI plays an important role in the field-dependent switching of magnetization and possible topological spin textures as a result of the competition between iDMI and IEC.

For Ru(7.1) film, the usual slanted hysteresis loop is observed and the field-descending curve [Fig. 3(a), solid black squares] is above the field-ascending curve [Fig. 3(a), solid black circles]. The magnetization is saturated at around 800 Oe and has a relative remanence of 0.15. At Ru thickness of 9.6 Å, the saturation field increases rapidly to 3130 Oe [Fig. 3(b)]. Starting from −3000 Oe (ascending curve), the system gradually switches from an aligned state to the $R_H \approx -0.4$ state, followed by a relatively sharp flip to the $R_H \approx -0.2$ state at −1790 Oe. From −1790 to 0 Oe, the system slowly transitions to the $R_H \approx 0$ state. In this process, coherent rotation of magnetization or realization of topological spin textures may occur. The system stays at the $R_H \approx 0$ state as the field increases from 0 to 1330 Oe. The system gradually switches to the $R_H \approx 0.4$ state (instead of the $R_H \approx 0.2$ state) from 1330 to 1840 Oe, then switches from the $R_H \approx 0.4$ state to an aligned state. Importantly, this hysteresis loop shows clear loop crossing between 1800 and 2000 Oe. Interestingly, the minor loop [Fig. 3(b), open blue triangle] does not overlap with the major loop and does not show loop crossing. The *nonzero* minor loop shift H_{MLS}, which is another signature of AFM-IEC and reflects the exchange field (i.e., magnitude of AFM-IEC), is around 2800 Oe, which is compatible to the iDMI field in Pt/Co/Ru [32].

As Ru thickness increases to 12 Å [Fig. 3(c)], AFM-IEC decreases and the saturation field decreases to 1700 Oe. A switching from zero magnetizing occurs at 400 Oe and H_{MLS} is around 1200 Oe. There is no loop crossing and the minor loop nearly overlaps with the major loop. At Ru thickness of 15.4 Å, ferromagnetic IEC is observed [Fig. 3(d)]. The saturation field is about 770 Oe and the relative remanence is close to 1. The AFM-IEC (i.e., resistance plateau and minor loop shift) resurges as Ru thickness further increases to 20.3 Å [Fig. 3(e)]. The minor loop matches perfectly with major loop with H_{MLS} around 300 Oe. When the Ru thickness increases to 23.8 Å, ferromagnetic IEC is observed [inset of Fig. 3(e)] and the remanence is close to 1.

Figures 3(a)–3(e) show how the oscillatory IEC is tuned by Ru thickness in $[Pt/Co/Ru(wedge)]_{10}$. As mentioned previously, Co layers are separated by Ru/Pt (i.e., Co/Ru/Pt/Co). Our results show that Pt does not block IEC originating from Ru. To study how the Pt layer affects IEC, we fabricated $[Pt(wedge)/Co(8)/Ru(7)]_{10}$ film. Figure 3(f) shows the normalized Hall loop of a $[Pt(5.9)/Co(8)/Ru(7)]_{10}$ film that is cut from a $[Pt(wedge)/Co(8)/Ru(7)]_{10}$ film. The Hall loop shows clear AFM-IEC with significant loop crossing from 2500 to 4000 Oe. The loop crossing is similar to an inverted hysteresis loop that gives negative remanence at zero field. Inverted hysteresis (negative remanence) has been observed in systems with competition between different magnetic energies [34], single-domain particles with two uniaxial anisotropies [35], and helical magnets (Fe,Co)Si [36] that host skyrmions. In our wedged films, only thickness of one nonmagnetic metal (Pt or Ru) varies. In this way, PMA and iDMI are expected to be unchanged in a single wedge film. In addition, there are no reports about the loop crossing for films with PMA and iDMI or films with PMA and IEC. Therefore, the loop crossing in Pt/Co/Ru(Ir) is very likely due to competition between iDMI and large AFM-IEC and requires further studies (e.g., detailed micromagnetic simulations). Note that simulations show that an inverted hysteresis loop is also found in the nucleation of skyrmions in magnetic nanodisks with iDMI [37].

In the multilayer films with IEC, the saturation field H_S overcomes the interlayer exchange field and is closely related to the magnitude of IEC. To (semi)quantitatively investigate the thickness dependence of IEC on nonmagnetic metals, we plot H_S as a function of thickness of Ru/Pt/Ir. Figure 4(a) shows H_S as a function of Ru thickness for various Ru wedge films with different Co thickness and repetition numbers. H_S oscillates with Ru thickness. As mentioned previously, we use two signatures (resistance plateau and minor loop shift) to identify AFM-IEC. For all the Ru wedge films, the first AFM-IEC peak occurs at around 9.5 Å, while the second one occurs at around 20 Å, giving a period of 10.5 Å. Because of the Pt layer, the first peak occurs at 9.5 Å instead of 3 Å in $[Co/Ru]_N$ multilayer films [19], but the period remains the

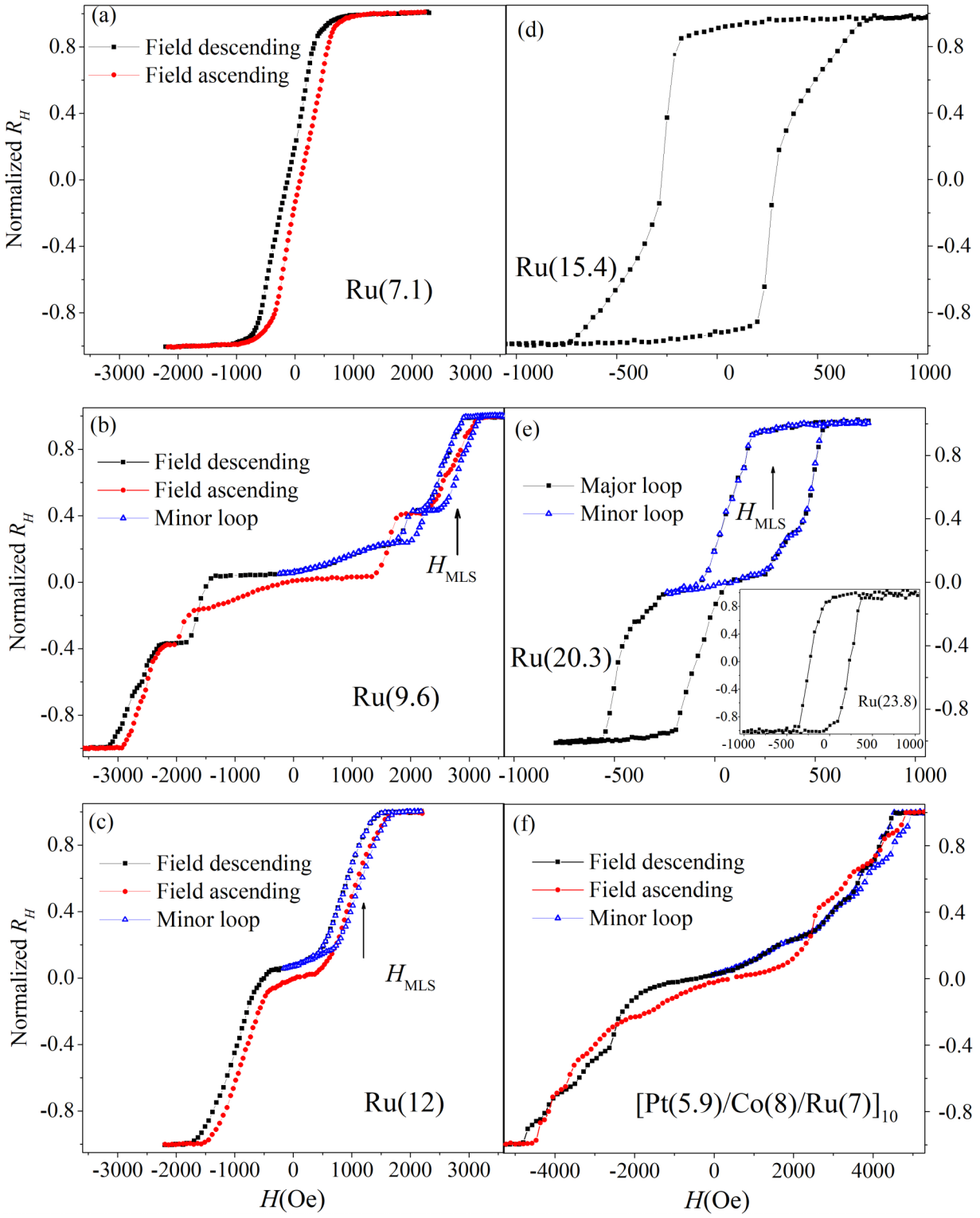

FIG. 3. (a)–(e) Normalized Hall resistance of $[Pt(10)/Co(8)/Ru(wedge)]_{10}$ superlattices as a function of magnetic field for field descending (solid black squares), field ascending (solid red circles), and minor loop (open blue triangles), respectively. Inset of (e) is for sample $[Pt(10)/Co(10)/Ru(23.8)]_{10}$. (f) Normalized Hall resistance loop for $[Pt(wedge)/Co(8)/Ru(7)]_{10}$ with Pt thickness of 5.9 Å.

same (about 11 Å), suggesting that the IEC originates from Ru. For Ru thickness between 7 and 12 Å where the AFM-IEC phase occurs, H_S varies sensitively with Ru thickness. The maximum H_S is around 4 kOe, corresponding to J_{AF} of $1.3\,mJ/m^2$ if $J_{AF} = H_S M_S t_F/4$ is adapted [19], where M_S is the saturation magnetization and t_F is the total Co thickness. The magnitude of J_{AF} is much weaker for the second AFM-IEC phase region. Most interestingly, the loop crossing only

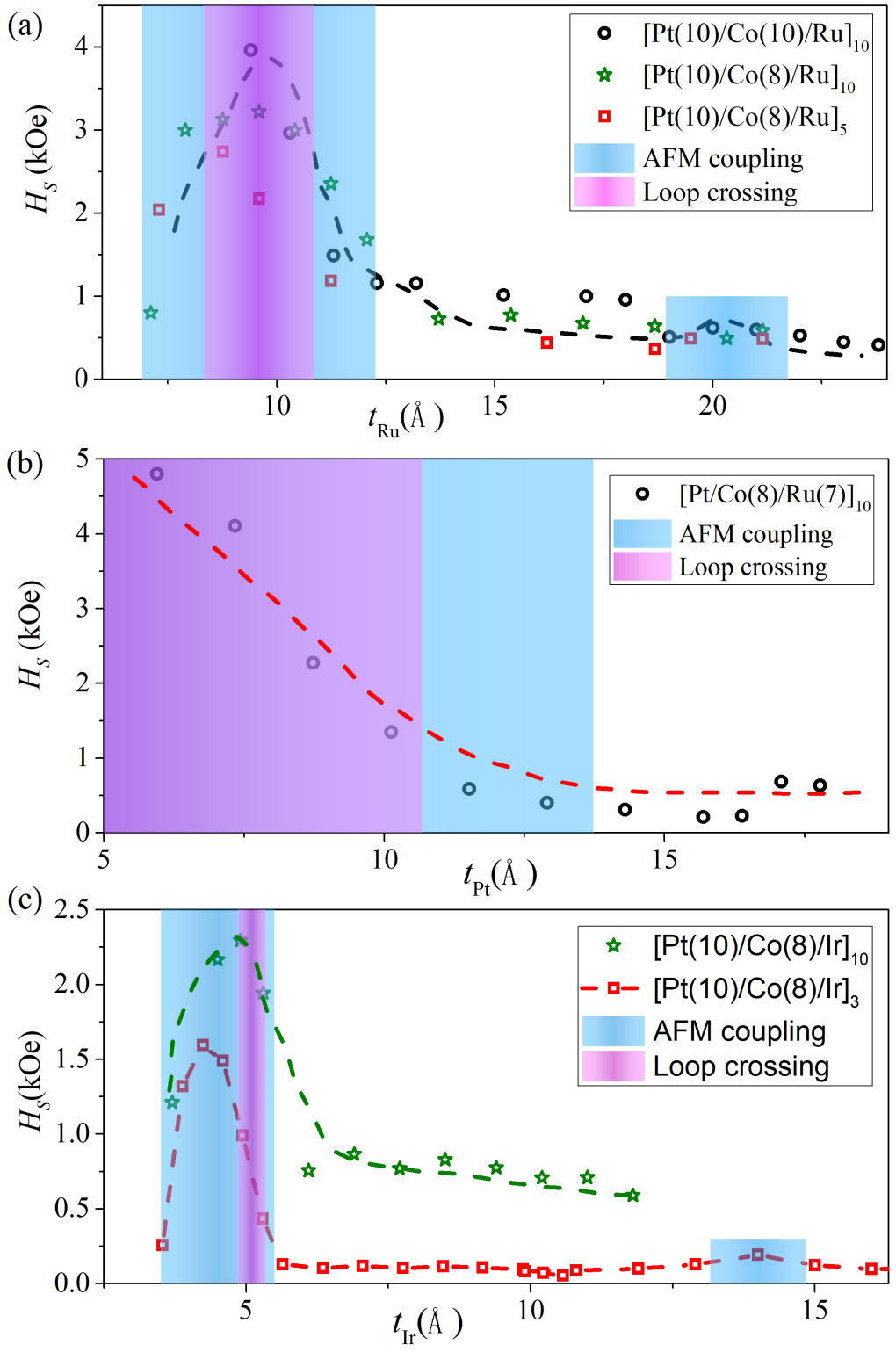

FIG. 4. Magnetic phase diagrams for (a) [Pt/Co/Ru(wedge)]$_N$, (b) [Pt(wedge)/Co(8)/Ru(7)]$_{10}$, and (c) [Pt/Co/Ir(wedge)]$_N$ superlattices. Dashed lines are guides to the eyes.

occurs at Ru thickness between 8.5 and 11 Å, in contrast to the wider and multiple phase regions of AFM-IEC.

Figure 4(b) shows H_S as a function of Pt thickness for [Pt(wedge)/Co(8)/Ru(7)]$_{10}$ films. The maximum H_S is around 4800 Oe, corresponding to J_{AF} of 1.2 mJ/m^2. In contrast to Ru wedge films, Pt wedge films do not show oscillatory IEC. H_S decreases monotonically as Pt thickness increases from 5.9 to 11.5 Å. AFM-IEC occurs at Pt thickness less than 13.7 Å, while the loop crossing only occurs at Pt thickness less than 10.7 Å. These results suggest that the Pt

layer acts as an effective "diluting" medium to tune AFM-IEC monotonically.

iDMI and magnetic skyrmions in Pt/Co/Ir multilayer films have been extensively studied. In this work, we systematically investigate IEC in Pt/Co/Ir(wedge) multilayer films [Fig. 4(c)]. Oscillatory IEC is also observed. The first peak of AFM-IEC occurs at Ir thickness of 4.5 Å that agrees with the value (4 Å) in $[Co/Ir]_N$ [19]. The second peak occurs at 14 Å and the period of oscillation is about 9.5 Å that is also close to the value (9 Å) in $[Co/Ir]_N$ [19]. The AFM-IEC occurs at Ir thickness from 3.5 to 5.5 Å and from 13.2 to 14.8 Å. However, loop crossing only occurs at a very narrow region of Ir thickness from 4.9 to 5.3 Å.

In magnetic multilayer films, in addition to Heisenberg exchange interaction, many other interactions can be introduced. PMA tends to align spins out of plane. iDMI tends to align neighboring spins perpendicular to each other. Both PMA and iDMI originate from the interface between FM and NM and can induce Néel skyrmions. In contrast to PMA and iDMI, IEC is mediated by an NM spacer between two FM layers (Fig. 1) and tends to align FM layers (or domains) in parallel or antiparallel ways. The IEC may act as a knob to fine tune topological spin textures and/or realize elusive antiferromagnetic skyrmions, especially when large IEC plays a different role (i.e., interlayer coupling) in conjunction with PMA and iDMI that are mediated by interface effects.

In summary, we systematically introduce IEC into Pt/Co/Ru(Ir) superlattices that have PMA and large iDMI. While PMA and iDMI are nearly independent on $t_{Ru/Ir}$ and t_{Pt} due to their interfacial nature, IEC is largely tunable by $t_{Ru/Ir}$ and t_{Pt}. The AFM-IEC is as large as about $1.3\,mJ/m^2$, on the same scale of iDMI. In addition, significant hysteresis loop crossing is observed when there is large AFM-IEC. More importantly, magnetic phase diagrams for AFM-IEC and unusual loop crossing are identified as a function of the thickness of nonmagnetic metals. Our experimental findings open a way to explore synthetic antiferromagnetic spintronics and antiferromagnetic skyrmions in which IEC will play an important role.

Work at the University of California at Davis was supported by the NSF Grant No. DMR-1610060 and at Georgetown University by the NSF Grant No. DMR-1905468.

[1] S. Mühlbauer, B. Binz, F. Jonietz, C. Pfleiderer, A. Rosch, A. Neubauer, R. Georgii, and P. Böni, Skyrmion lattice in a chiral magnet, Science **323**, 915 (2009).

[2] W. Jiang, G. Chen, K. Liu, J. Zang, S. G. E. te Velthuis, and A. Hoffmann, Skyrmions in magnetic multilayers, Phys. Rep. **704**, 1 (2017).

[3] L. Sun, R. X. Cao, B. F. Miao, Z. Feng, B. You, D. Wu, W. Zhang, A. Hu, and H. F. Ding, Creating an Artificial Two-Dimensional Skyrmion Crystal by Nanopatterning, Phys. Rev. Lett. **110**, 167201 (2013).

[4] D. A. Gilbert, B. B. Maranville, A. L. Balk, B. J. Kirby, P. Fischer, D. T. Pierce, J. Unguris, J. A. Borchers, and K. Liu, Realization of ground-state artificial skyrmion lattices at room temperature, Nat. Commun. **6**, 8462 (2015).

[5] J. Li, A. Tan, K. W. Moon, A. Doran, M. A. Marcus, A. T. Young, E. Arenholz, S. Ma, R. F. Yang, C. Hwang, and Z. Q. Qiu, Tailoring the topology of an artificial magnetic skyrmion, Nat. Commun. **5**, 4704 (2014).

[6] J. Sampaio, V. Cros, S. Rohart, A. Thiaville, and A. Fert, Nucleation, stability and current-induced motion of isolated magnetic skyrmions in nanostructures, Nat. Nano **8**, 839 (2013).

[7] C. Moreau-Luchaire, C. Moutafis, N. Reyren, J. Sampaio, C. A. F. Vaz, N. Van Horne, K. Bouzehouane, K. Garcia, C. Deranlot, P. Warnicke, P. Wohlhüter, J.-M. George, M. Weigand, J. Raabe, V. Cros, and A. Fert, Additive interfacial chiral interaction in multilayers for stabilization of small individual skyrmions at room temperature, Nat. Nano **11**, 444 (2016).

[8] S. Woo, K. Litzius, B. Kruger, M.-Y. Im, L. Caretta, K. Richter, M. Mann, A. Krone, R. M. Reeve, M. Weigand, P. Agrawal, I. Lemesh, M.-A. Mawass, P. Fischer, M. Klaui, and G. S. D. Beach, Observation of room-temperature magnetic skyrmions and their current-driven dynamics in ultrathin metallic ferromagnets, Nat. Mater. **15**, 501 (2016).

[9] W. Jiang, P. Upadhyaya, W. Zhang, G. Yu, M. B. Jungfleisch, F. Y. Fradin, J. E. Pearson, Y. Tserkovnyak, K. L. Wang, O. Heinonen, S. G. E. te Velthuis, and A. Hoffmann, Blowing magnetic skyrmion bubbles, Science **349**, 283 (2015).

[10] A. Soumyanarayanan, M. Raju, A. L. Gonzalez Oyarce, A. K. C. Tan, M.-Y. Im, A. P. Petrovic, P. Ho, K. H. Khoo, M. Tran, C. K. Gan, F. Ernult, and C. Panagopoulos, Tunable room-temperature magnetic skyrmions in Ir/Fe/Co/Pt multilayers, Nat. Mater. **16**, 898 (2017).

[11] H. S. Park, X. Yu, S. Aizawa, T. Tanigaki, T. Akashi, Y. Takahashi, T. Matsuda, N. Kanazawa, Y. Onose, D. Shindo, A. Tonomura, and Y. Tokura, Observation of the magnetic flux and three-dimensional structure of skyrmion lattices by electron holography, Nat. Nano **9**, 337 (2014).

[12] A. K. Nayak, V. Kumar, T. Ma, P. Werner, E. Pippel, R. Sahoo, F. Damay, U. K. Rößler, C. Felser, and S. S. P. Parkin, Magnetic antiskyrmions above room temperature in tetragonal Heusler materials, Nature (London) **548**, 561 (2017).

[13] M. Hoffmann, B. Zimmermann, G. P. Müller, D. Schürhoff, N. S. Kiselev, C. Melcher, and S. Blügel, Antiskyrmions stabilized at interfaces by anisotropic Dzyaloshinskii-Moriya interactions, Nat. Commun. **8**, 308 (2017).

[14] S. Huang, C. Zhou, G. Chen, H. Shen, A. K. Schmid, K. Liu, and Y. Wu, Stabilization and current-induced motion of antiskyrmion in the presence of anisotropic Dzyaloshinskii-Moriya interaction, Phys. Rev. B **96**, 144412 (2017).

[15] J. Barker and O. A. Tretiakov, Static and Dynamical Properties of Antiferromagnetic Skyrmions in the Presence of Applied Current and Temperature, Phys. Rev. Lett. **116**, 147203 (2016).

[16] X. Zhang, Y. Zhou, and M. Ezawa, Magnetic bilayer-skyrmions without skyrmion Hall effect, Nat. Commun. **7**, 10293 (2016).

[17] S. Woo, K. M. Song, X. Zhang, Y. Zhou, M. Ezawa, X. Liu, S. Finizio, J. Raabe, N. J. Lee, S.-I. Kim, S.-Y. Park, Y. Kim, J.-Y. Kim, D. Lee, O. Lee, J. W. Choi, B.-C. Min, H. C. Koo, and

J. Chang, Current-driven dynamics and inhibition of the skyrmion Hall effect of ferrimagnetic skyrmions in GdFeCo films, Nat. Commun. **9**, 959 (2018).

[18] L. Šmejkal, Y. Mokrousov, B. Yan, and A. H. MacDonald, Topological antiferromagnetic spintronics, Nat. Phys. **14**, 242 (2018).

[19] S. S. P. Parkin, Systematic Variation of the Strength and Oscillation Period of Indirect Magnetic Exchange Coupling Through the 3d, 4d, and 5d Transition Metals, Phys. Rev. Lett. **67**, 3598 (1991).

[20] P. J. H. Bloemen, H. W. van Kesteren, H. J. M. Swagten, and W. J. M. de Jonge, Oscillatory interlayer exchange coupling in Co/Ru multilayers and bilayers, Phys. Rev. B **50**, 13505 (1994).

[21] P. Bruno, Theory of interlayer magnetic coupling, Phys. Rev. B **52**, 411 (1995).

[22] M. D. Stiles, Interlayer exchange coupling, J. Magn. Magn. Mater. **200**, 322 (1999).

[23] R. A. Duine, K.-J. Lee, S. S. P. Parkin, and M. D. Stiles, Synthetic antiferromagnetic spintronics, Nat. Phys. **14**, 217 (2018).

[24] S. Parkin and S.-H. Yang, Memory on the racetrack, Nat. Nano **10**, 195 (2015).

[25] G. Chen, A. Mascaraque, A. T. Diaye, and A. K. Schmid, Room temperature skyrmion ground state stabilized through interlayer exchange coupling, Appl. Phys, Lett. **106**, 242404 (2015).

[26] A. K. Nandy, N. S. Kiselev, and S. Blügel, Interlayer Exchange Coupling: A General Scheme Turning Chiral Magnets into Magnetic Multilayers Carrying Atomic-Scale Skyrmions, Phys. Rev. Lett. **116**, 177202 (2016).

[27] E. van Walsem, R. A. Duine, J. Lucassen, R. Lavrijsen, and H. J. M. Swagten, Structural transitions of skyrmion lattices in synthetic antiferromagnets, arXiv:1812.08082.

[28] O. Hellwig, T. L. Kirk, J. B. Kortright, A. Berger, and E. E. Fullerton, A new phase diagram for layered antiferromagnetic films, Nat. Mater. **2**, 112 (2003).

[29] J. E. Davies, O. Hellwig, E. E. Fullerton, and K. Liu, Temperature-dependent magnetization reversal in (Co/Pt)/Ru multilayers, Phys. Rev. B **77**, 014421 (2008).

[30] N. S. Kiselev, C. Bran, U. Wolff, L. Schultz, A. N. Bogdanov, O. Hellwig, V. Neu, and U. K. Rößler, Metamagnetic domains in antiferromagnetically coupled multilayers with perpendicular anisotropy, Phys. Rev. B **81**, 054409 (2010).

[31] C. Bran, A. B. Butenko, N. S. Kiselev, U. Wolff, L. Schultz, O. Hellwig, U. K. Rößler, A. N. Bogdanov, and V. Neu, Evolution of stripe and bubble domains in antiferromagnetically coupled $[(Co/Pt)_8/Co/Ru]_{18}$ multilayers, Phys. Rev. B **79**, 024430 (2009).

[32] D. Khadka, S. Karayev, and S. X. Huang, Dzyaloshinskii-Moriya interaction in Pt/Co/Ir and Pt/Co/Ru multilayer films, J. Appl. Phys. **123**, 123905 (2018).

[33] H. Nemoto, H. Nakagawa, and Y. Hosoe, Dependence of Co/Pd superlattice properties on Pd layer thickness, IEEE Trans. Magn. **39**, 2714 (2003).

[34] M. Ziese, I. Vrejoiu, and D. Hesse, Inverted hysteresis and giant exchange bias in $La_{0.7}Sr_{0.3}MnO_3/SrRuO_3$ superlattices, Appl. Phys. Lett. **97**, 052504 (2010).

[35] Y. Jae Nam and S. H. Lim, Negative remanent magnetization in a single domain particle with two uniaxial anisotropies, Appl. Phys. Lett. **99**, 092503 (2011).

[36] M. K. Chattopadhyay, S. B. Roy, and S. Chaudhary, Magnetic properties of $Fe_{1-x}Co_xSi$ alloys, Phys. Rev. B **65**, 132409 (2002).

[37] A. G. Kolesnikov, A. S. Samardak, M. E. Stebliy, A. V. Ognev, L. A. Chebotkevich, A. V. Sadovnikov, S. A. Nikitov, Y. J. Kim, I. H. Cha, and Y. K. Kim, Spontaneous nucleation and topological stabilization of skyrmions in magnetic nanodisks with the interfacial Dzyaloshinskii–Moriya interaction, J. Magn. Magn. Mater. **429**, 221 (2017).